

Dynamic ductile to brittle transition in a one-dimensional model of viscoplasticity

Alexander E. Lobkovsky[†] and J. S. Langer[‡]

[†]*Institute for Theoretical Physics, University of California, Santa Barbara, CA 93106*

[‡]*Department of Physics, University of California, Santa Barbara, CA 93106*

(November 16, 2016)

We study two closely related, nonlinear models of a viscoplastic solid. These models capture essential features of plasticity over a wide range of strain rates and applied stresses. They exhibit inelastic strain relaxation and steady flow above a well defined yield stress. In this paper, we describe a first step in exploring the implications of these models for theories of fracture and related phenomena. We consider a one dimensional problem of decohesion from a substrate of a membrane that obeys the viscoplastic constitutive equations that we have constructed. We find that, quite generally, when the yield stress becomes smaller than some threshold value, the energy required for steady decohesion becomes a non-monotonic function of the decohesion speed. As a consequence, steady state decohesion at certain speeds becomes unstable. We believe that these results are relevant to understanding the ductile to brittle transition as well as fracture stability.

I. INTRODUCTION

A wide range of evidence points toward the necessity of including plastic deformation near a crack tip among the relevant degrees of freedom in theories of dynamic brittle fracture. Our own ideas about this issue emerge from our recent attempt to study fracture stability using a class of cohesive-zone models in which such deformations are necessarily absent. As described in our report on this project [1], we discovered both mathematical and physical difficulties that, so far as we could tell, can be overcome only by introducing tip blunting or, perhaps, a spatially extended process zone in which irreversible deformations of the brittle solid are taking place.

A successful theory of dynamic fracture also must explain failure of materials that can flow plastically. Stroh [2] understood that cleavage in such materials is an inherently dynamic process in which plastic flow is slow enough that stresses can increase to large values near the crack tip. In order to explain slower ductile crack propagation, McClintock [3] introduced a novel void nucleation and coalescence mechanism. At present, theories of these two failure mechanisms are separate and incompatible with one another.

Attempts to explain the differences between ductile to brittle fracture usually focus on the emission and mobility of dislocations near the crack tip [4,5]. A different microscopic mechanism must be responsible for the ductile to brittle transition in noncrystalline materials such as toughened thermoplastics [6,7]. The study of Freund and Hutchinson aimed at understanding dynamic fracture within a theory of continuum plasticity [8,9]. Under the assumption of elastic strain-rate dominance near the tip, they found a non-monotonic dependence of the fracture toughness on the crack speed. They used an idealized viscoplastic constitutive law, however, in which the plastic strain rate is identically zero below a yield stress and responds instantaneously to changes in the stress. The condition of elastic strain-rate dominance

breaks down for slow cracks, and thus the analysis of Freund and Hutchinson cannot be generally valid. A different approach by Freund's [10] has been to use a rate-dependent cohesive-zone model [11] and to consider two separate fracture criteria, one based on stress and the other on displacement. This is the class of models that we found to be ill-posed for our stability analyses, presumably because they omit essential features of an extended plastic process zone.

In a recent study, M. L. Falk and one of the present authors (JSL) have proposed a theory of viscoplasticity in amorphous materials [12] (denoted FL in what follows) in which the equations of linear elastodynamics are supplemented by nonlinear equations of motion for a set of internal state variables. This theory is based directly on molecular-dynamics simulations which revealed the existence of localized weak regions, called "shear transformation zones." The new internal state variables describe the populations of these zones, and the nonlinear equations describe how those populations determine the time-dependent elastic and plastic behavior of the material.

In the picture presented in FL, the shear transformation zones are two-state systems, and transitions between those states produce increments in the plastic strain. Because a zone that has transformed once cannot transform again in the same direction, the plastic strain remains bounded when the applied stress is small. An additional assumption of FL is that the zones are created and annihilated at rates determined by the inelastic shear rate. It is this process, in which new zones replace old ones, that produces persistent plastic flow at sufficiently large stresses. Plasticity is a fully dynamic phenomenon in this theory. It occurs in a well defined way, depending on the state of the system, in response to time dependent perturbations. Thus this new theory may be capable of describing both brittleness and ductility in fracture.

We report here on our initial attempts to incorporate some of the basic features of the FL theory into a model of fracture. As a first step in exploring the implications

of this theory, we examine a one-dimensional model of decohesion of a thin membrane from a substrate, where the membrane obeys a simplified version of the FL viscoplastic constitutive equations. The membrane is pulled from the substrate by weak springs, and the point of decohesion propagates at constant speed, like a crack tip. As noted by Barber *et. al.* [13] and Marder and Gross [14], the inverse stiffness of the driving springs in such models is analogous, at least in some ways, to the width of the strip in two-dimensional mode-I fracture. This effective width plays an important role in our interpretation of the brittle-ductile transition in this system. The one-dimensional nature of the model is, of course, a significant limitation.

This article is organized as follows. We introduce our simplified FL model in Section II. In particular, we introduce two different versions of the nonlinear term that determines the plastic yield stress, and we examine the time dependence of the system near the onset of plastic flow for these two cases. In Section III, we discuss the linear version of this model and show that it corresponds to conventional viscoelasticity with inelastic deformation but no persistent plastic flow. Then, in Section IV, we describe both analytic and numerical studies of the nonlinear model, and show how the two rate-dependent mechanisms introduced in Section II produce different versions of a brittle-ductile transition. We conclude in Section V with a discussion of how the lessons learned from this simple class of models might be applicable to more realistic situations.

II. ONE-DIMENSIONAL MODEL OF DECOHESION

We consider a thin membrane decohering from a substrate as shown in Fig. 1. The system has translational symmetry in the direction perpendicular to the plane of the Figure. As an additional simplifying approximation, we allow the membrane to move only in the direction perpendicular to the substrate. The configuration of the membrane is thus described by its displacement $u(x, t)$, a non-negative function of position x and time t . A cohesive force,

$$f = \begin{cases} -\kappa^2 u & \text{for } 0 < u < \delta \\ 0 & \text{otherwise,} \end{cases} \quad (2.1)$$

with a finite range δ , attracts the membrane to the substrate. Decohesion is driven by weak springs of strength α^2 whose relaxed positions are at $u = u_\infty$. The total strain in the membrane is $\epsilon_{tot} = \partial u / \partial x$. This strain and, equivalently, the displacement u consist of additive elastic and plastic parts:

$$u = u_{el} + u_{pl}; \quad \epsilon_{tot} = \frac{\partial u_{el}}{\partial x} + \frac{\partial u_{pl}}{\partial x}. \quad (2.2)$$

For later notational simplicity, we write

$$\frac{\partial u_{pl}}{\partial x} = \epsilon. \quad (2.3)$$

By definition, the elastic part of the strain is linearly proportional to the stress, $\sigma = 2\mu(\partial u_{el} / \partial x)$, where μ is the shear modulus. Then the equation of motion for the membrane is

$$\rho \ddot{u} = \frac{\partial \sigma}{\partial x} - \kappa^2 u \Theta(\delta - u) - \alpha^2 (u - u_\infty), \quad (2.4)$$

where ρ is the linear mass density and $\Theta(\cdot)$ is the Heaviside step function. Dots denote time derivatives.

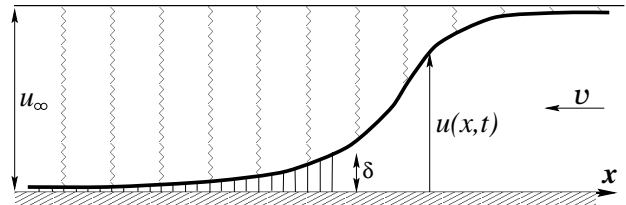


FIG. 1. A model of one dimensional decohesion driven by weak springs.

The equation of motion for the plastic strain that we shall use here is:

$$\dot{\epsilon} = \frac{1}{\tau} (\lambda \sigma - \Delta). \quad (2.5)$$

This is a simplified version of Eq. (3.14) in FL. (We have evaluated the right-hand side of the latter equation in the limit of small stress σ and have set $n_\Delta = \Delta$, $n_{tot} = n_\infty$.) By making this small- σ approximation, we lose some of the memory effects that were obtained in FL via a strongly nonlinear σ -dependence of the rate factors in the equation for $\dot{\epsilon}$. We believe that the absence of those effects makes only quantitative and not qualitative differences in the results to be presented here. However, that point may require further investigation.

Our single state variable, $\Delta(x, t)$, is a measure of the imbalance in the populations of the two-state systems. The first term on the right-hand side of (2.5), $\lambda \sigma / \tau$, is the usual linear relation between the plastic strain rate and the stress. The second term, $-\Delta / \tau$, is the rate at which these two-state systems transform spontaneously from their “forward” to their “backward” states, and is therefore a negative contribution to $\dot{\epsilon}$.

Our equation of motion for Δ has the form:

$$\dot{\Delta} = \dot{\epsilon} - \mathcal{F}(\dot{\epsilon}, \sigma) \Delta. \quad (2.6)$$

This is exactly the same as Eq. (3.15) in FL except that we have not yet specified the strain-rate dependent coupling \mathcal{F} between $\dot{\Delta}$ and Δ . The first term on the right hand side of (2.6) simply expresses our assumption that the transitions within the two-state systems correspond to increments in plastic strain. The second, i.e. the nonlinear term, is the effect of creation and annihilation of

these zones and, as we shall see immediately, is responsible for the existence of a finite plastic yield stress.

To illustrate the properties of the nonlinear term in (2.6), we consider two plausible forms of \mathcal{F} that produce qualitatively different dynamic decohesion in certain regimes. The form of \mathcal{F} is restricted by the assumption that it must vanish when the plastic strain rate vanishes. It is thus proportional to some power of $\dot{\epsilon}$. (In higher dimensions, we would also require rotational invariance.) The first form that we shall examine is the same as that used in FL: $\mathcal{F}_1 = \gamma_1 \dot{\epsilon} \sigma$. Here, the coupling \mathcal{F}_1 is proportional to the local rate of plastic energy dissipation. We call this Model 1. Note that \mathcal{F}_1 can be negative in some circumstances. Our second possibility, Model 2, is one in which only the local plastic strain rate controls the evolution of Δ , in which case the simplest choice is $\mathcal{F}_2 = \gamma_2 \dot{\epsilon}^2$.

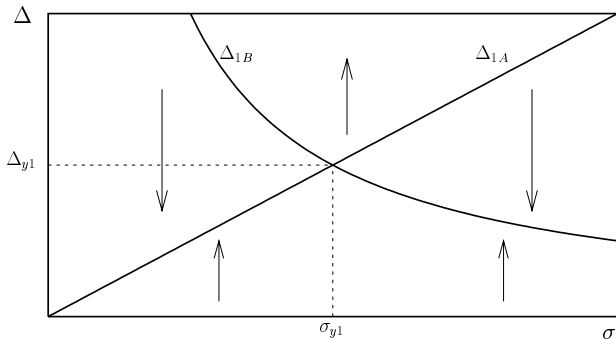


FIG. 2. The steady state values of Δ in Model 1 as functions of σ . The two curves $\Delta_{1A} = \lambda\sigma$ and $\Delta_{1B} = 1/\gamma_1\sigma$ cross at $(\sigma_{y1}, \Delta_{y1})$. The arrows indicate the direction of motion of Δ for fixed σ .

We explore first the behavior of Model 1. Substituting the expression for $\dot{\epsilon}$ from (2.5) into (2.6), we obtain

$$\dot{\Delta} = \frac{1}{\tau} (\lambda\sigma - \Delta) (1 - \gamma_1\sigma\Delta). \quad (2.7)$$

For constant stress σ , there are two stationary solutions:

$$\Delta = \Delta_{1A} = \lambda\sigma, \quad \text{and} \quad \Delta = \Delta_{1B} = \frac{1}{\gamma_1\sigma}, \quad (2.8)$$

which, as shown in Figure 2, cross at

$$\sigma = \sigma_{y1} = \frac{1}{\sqrt{\gamma_1\lambda}}, \quad \Delta = \Delta_{y1} = \sqrt{\frac{\lambda}{\gamma_1}}. \quad (2.9)$$

At any fixed σ , only one of these stationary solutions is stable against perturbations. For $\sigma < \sigma_{y1}$, the stationary solution Δ_{1A} with $\dot{\epsilon} = 0$ is stable. For $\sigma > \sigma_{y1}$, on the other hand, the stable stationary solution $\Delta = \Delta_{1B}$ is a flowing steady state with

$$\dot{\epsilon} = \frac{\lambda}{\sigma\tau} (\sigma^2 - \sigma_{y1}^2). \quad (2.10)$$

This rate vanishes when the stress approaches yield from above. However, the relaxation time τ_1 for perturbations away from the flowing state diverges for σ near σ_{y1} :

$$\tau_1 = \frac{\sigma_{y1}^2 \tau}{|\sigma^2 - \sigma_{y1}^2|}. \quad (2.11)$$

This is quite unlike the conventional elastic-ideally plastic solid in which this relaxation time is zero by definition.

A possibly unphysical feature of this model is that, for some initial conditions, Δ may increase indefinitely as a function of time. It is easy to see from (2.7), however, that if $\Delta < \Delta_{y1}$ at any time, it will remain so for all other times regardless of the stress history.

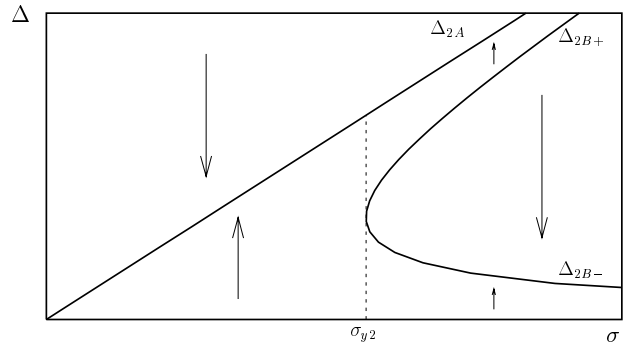


FIG. 3. Steady state values of Δ as functions of σ for Model 2. One of the three, Δ_{2B+} , is unstable to small perturbations. Since the steady state curves never cross, the system remains close to the non-flowing steady state Δ_{2A} if the stress increases slowly enough. The meaning of the arrows is the same as in Fig. 2.

Model 2 exhibits an important qualitative difference in its behavior. Let us perform the analysis of the preceding paragraphs using \mathcal{F}_2 . Substituting (2.5) into (2.6), we obtain

$$\dot{\Delta} = \frac{1}{\tau} (\lambda\sigma - \Delta) \left(\frac{\gamma_2}{\tau} \Delta^2 - \frac{\gamma_2 \lambda \sigma}{\tau} \Delta + 1 \right). \quad (2.12)$$

We again look for the stationary states $\dot{\Delta} = 0$. The situation is shown in Fig. 3. In this case, the state with $\Delta = \Delta_{2A} = \lambda\sigma$ and no plastic flow, $\dot{\epsilon} = 0$, is stable for all σ . As seen in Fig. 3, it never intersects any other state in the Δ - σ plane. For

$$\sigma > \sigma_{y2} = \frac{2}{\lambda} \sqrt{\frac{\tau}{\gamma_2}}, \quad (2.13)$$

two new stationary states appear with

$$\Delta = \Delta_{2B\pm} = \frac{\lambda}{2} \left(\sigma \pm \sqrt{\sigma^2 - \sigma_{y2}^2} \right). \quad (2.14)$$

The state with $\Delta = \Delta_{2B-}$ is the stable one of the pair. The plastic strain rate in this stationary state is non-zero:

$$\dot{\epsilon} = \frac{\lambda}{2\tau} \left(\sigma + \sqrt{\sigma^2 - \sigma_{y2}^2} \right). \quad (\text{steady state, } \sigma > \sigma_{y2}). \quad (2.15)$$

The characteristic decay time τ_2 of perturbations around the flowing stationary state again diverges at the yield stress, although the divergence is not as strong as in Model 1:

$$\tau_2 = \frac{\tau}{2} \frac{\sigma_{y2}^2}{\left(\sigma + \sqrt{\sigma^2 - \sigma_{y2}^2} \right) \sqrt{\sigma^2 - \sigma_{y2}^2}}, \quad (\sigma > \sigma_{y2}). \quad (2.16)$$

The two nonlinear models exhibit a number of similar features. Most importantly, steady plastic flow in response to a stress above a yield level is a natural consequence of the dynamical constitutive equations. The flow has a non-zero response time to changes in the stress. It can also be shown that inelastic strain is partially recovered in both models. However, there are several important differences between the two nonlinear models. First, the steady flow rate does not vanish in Model 2 at $\sigma = \sigma_{y2}$. Second, “runaway” behavior cannot occur in that model since $\dot{\Delta} < 0$ for $\Delta > \Delta_{2A}$. And finally, for stresses greater than the yield stress, there are two stable stationary solutions in Model 2 as opposed to only one in Model 1. Which one of these is selected by the system depends on the stress history. For example, only the non-flowing state in Model 2, with $\Delta = \Delta_{2A}$, occurs if the stress is increased slowly enough, i.e. when $\dot{\sigma}/\sigma \ll 1/\tau$. As we shall see, this distinction between the models leads to qualitatively different behaviors at small speeds.

It is convenient at this point to convert to dimensionless variables in which all lengths are measured in units of the range of the cohesive interaction δ , time is measured in units of $\delta\sqrt{\rho/2\mu}$, and stress in units of 2μ . For simplicity, we continue to use the symbols u and σ for our dimensionless displacements and stresses. We also restrict our attention to steady-state solutions moving in the negative x direction with speed v . All functions of x and t in the frame of reference moving with the decohesion front depend only on the combination $x' = x + vt$. Without loss of generality, we set $x' = 0$ at the point of decohesion where, in these units, $u = 1$. Then, for simplicity, we set $x' = x$.

Our equations of motion now have the form:

$$v^2(u_{el}'' + u_{pl}'') = u_{el}'' - \kappa^2(u_{el} + u_{pl})\Theta(-x) - \alpha^2(u_{el} + u_{pl} - u_\infty), \quad (2.17)$$

$$vu_{pl}'' = \frac{1}{\tau}(\lambda u_{el}' - \Delta), \quad (2.18)$$

$$v\Delta' = vu_{pl}'' - \mathcal{F}(vu_{pl}'', u_{el}')\Delta, \quad (2.19)$$

where primes denote differentiation with respect to x , and

$$\mathcal{F}_1 = \gamma_1 vu_{pl}'' u_{el}'; \quad (2.20)$$

$$\mathcal{F}_2 = \gamma_2 (vu_{pl}'')^2. \quad (2.21)$$

Finally, we derive an expression for the decohesion resistance $G(v)$, which is the work that the driving springs perform on the membrane per unit length of advance of the decohesion front. Since the driving springs relax to their equilibrium length far behind the decohesion front, all of their stored elastic energy ahead of the front must be dissipated in the decohesion process. Thus, the total work done must be

$$G(v) = \frac{1}{2} \alpha^2 u_\infty^2. \quad (2.22)$$

If we multiply (2.17) by $u'(x)$ and integrate over x , we obtain

$$G(v) = \frac{1}{2} \kappa^2 + \int dx u_{pl}'' u_{el}' + \frac{1}{2} (u_{pl}')^2 \Big|_{x=\infty}. \quad (2.23)$$

The first term on the right-hand side of (2.23) is clearly the energy spent in breaking cohesive bonds. The second term is the energy dissipated in plastic work in the neighborhood of the decohesion front. The third term is the energy locked into the plastic wake left by the decohesion. The decohesion front in this model may leave a residual plastic strain behind it. Our problem is to compute $G(v)$ explicitly as a function of v and then use (2.22) to determine v as a function of the driving force αu_∞ .

III. LINEAR ANALYSIS

Before going ahead with an analysis of this nonlinear model of viscoplasticity, it will be useful to look briefly at the linear case in which we set $\mathcal{F} = 0$ in (2.6). Then we have $\Delta = \epsilon = u_{pl}'$; and the equation of motion for u_{pl} is

$$\dot{u}_{pl} = vu_{pl}' = \frac{1}{\tau}(\lambda u_{el} - u_{pl}). \quad (3.1)$$

The remaining equation of motion is (2.4) or, equivalently, (2.17).

Far away from the region where decohesion is taking place, our system is translationally invariant, and we can compute a dispersion relation for waves of the form $u = u_0 \exp(ikx - i\omega_k t)$. In the limit of vanishing α , we find

$$k^2 = \omega_k^2 \left(1 + \frac{\lambda}{1 - i\omega_k \tau} \right). \quad (3.2)$$

The wave speed c is

$$c \equiv \lim_{k \rightarrow 0} \text{Re} \frac{\omega_k}{k} = \frac{1}{\sqrt{1 + \lambda}}. \quad (3.3)$$

It is important to recognize that, by linearizing, we have reduced our system to a conventional model of viscoelasticity. The solution of the time-dependent version of (3.1) can be written in the familiar form

$$\epsilon_{tot}(t) = \frac{1}{c^2} \sigma(t) - \lambda \int_{-\infty}^t dt' \exp \left[-\frac{1}{\tau}(t - t') \right] \dot{\sigma}(t') \quad (3.4)$$

where ϵ_{tot} is the total (elastic plus plastic) strain, and $\sigma = \partial u_{el}/\partial x$ is the stress in dimensionless units. Equivalently,

$$\sigma(t) = c^2 \epsilon_{tot}(t) + \lambda \int_{-\infty}^t dt' \exp\left[-\frac{1}{\tau c^2}(t-t')\right] \dot{\epsilon}_{tot}(t'). \quad (3.5)$$

From (3.4) we find that the creep compliance — the variation of the strain that is produced by a unit jump in the stress — is

$$C(t) = 1 + \lambda \left(1 - e^{-t/\tau}\right). \quad (3.6)$$

The system exhibits unit instantaneous elasticity, following which the strain increases on the time scale τ to its final value $1 + \lambda = 1/c^2$. Similarly, we see from (3.5) that a unit jump in the strain produces first an instantaneous jump in the stress, after which the stress decreases to a constant, nonzero value.

Because our equations of motion (2.17) and (3.1) are linear, we can solve the decohesion problem analytically. (We shall need these linear solutions in order to interpret features of the nonlinear solutions described in the next Section.) The analysis is particularly simple if we take the limit of weak driving springs, $\alpha \rightarrow 0$. To do this, we must also take the limit $u_\infty \rightarrow \infty$ in such a way as to keep αu_∞ constant. That is, we keep $G(v)$ fixed in (2.22).

For $x < 0$, we can set $\alpha = 0$ immediately in (2.17) and look for a solution in the form:

$$u_{el} = A e^{qx}, \quad u_{pl} = B e^{qx}. \quad (3.7)$$

That is, we look for values of A , B , and q that satisfy the homogeneous equation:

$$\begin{pmatrix} -\beta^2 q^2 + \kappa^2 & v^2 q^2 + \kappa^2 \\ -\lambda/v\tau & q + 1/v\tau \end{pmatrix} \begin{pmatrix} A \\ B \end{pmatrix} = 0. \quad (3.8)$$

The solvability condition for (3.8) is:

$$q^3 v\tau \beta^2 + q^2 \beta_c^2 - q v\tau \kappa^2 - \frac{\kappa^2}{c^2} = 0, \quad (3.9)$$

where

$$\beta^2 \equiv 1 - v^2; \quad \beta_c^2 \equiv 1 - v^2/c^2. \quad (3.10)$$

Eq. (3.9) has only one positive root, say q_1 . The boundary condition $u_{el}(0) + u_{pl}(0) = 1$ is therefore sufficient to determine uniquely the solution in the region $x < 0$. We find:

$$A = c^2 \left(\frac{1 + q_1 v\tau}{1 + q_1 v\tau c^2} \right); \quad B = \frac{\lambda c^2}{1 + q_1 v\tau c^2}. \quad (3.11)$$

For $x > 0$, all κ 's appearing in (3.9) must be replaced by α 's. The resulting equation has two negative solutions for q which, for small α , are:

$$q_0 = -\frac{\alpha}{\beta_c c}; \quad q_2 = -\frac{\beta_c^2}{v\tau \beta^2} + \mathcal{O}(\alpha^2). \quad (3.12)$$

We therefore construct solutions of the form:

$$u_{el} = D_1 e^{q_0 x} + D_2 e^{q_2 x} + c^2 u_\infty, \quad (3.13)$$

$$u_{pl} = \left(\frac{\lambda D_1}{1 + v\tau q_0} \right) e^{q_0 x} + \left(\frac{\lambda D_2}{1 + v\tau q_2} \right) e^{q_2 x} + (1 - c^2) u_\infty. \quad (3.14)$$

Here, we have included the particular solutions (simple constants) that satisfy the boundary condition $u \rightarrow u_\infty$ at $x \rightarrow +\infty$. We then require that u_{el} and u_{pl} and their derivatives be continuous at $x = 0$. Calculating to first order in αu_∞ , we find:

$$D_1 = -c^2 u_\infty \left(1 + \frac{q_0}{q_2} \right) + A \left(1 - \frac{q_1}{q_2} \right), \quad (3.15)$$

$$D_2 = A \frac{q_1}{q_2} + c^2 u_\infty \frac{q_0}{q_2}, \quad (3.16)$$

where A is given in (3.11). Finally,

$$K(v) \equiv \sqrt{2G(v)} = \alpha u_\infty = \frac{q_1 c}{\beta_c} \left(\frac{\beta^2 v\tau q_1 + \beta_c^2}{c^2 v\tau q_1 + 1} \right). \quad (3.17)$$

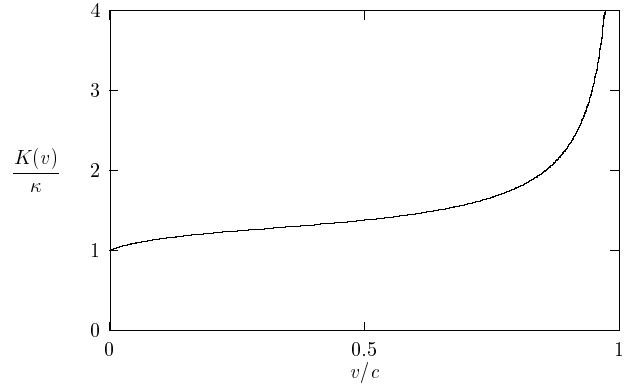


FIG. 4. Decohesion toughness $K(v)$ for the linear model with $\tau = 10$ and $\lambda = 1$.

We show a representative graph of K as a function of the speed v in Fig. 4. As expected from a model of this kind, $K(v)$ is monotonic, diverges at $v = c$ as $1/\beta_c$, and is equal to κ for $v = 0$, which confirms that viscous dissipation is negligible for slow decohesion.

IV. SOLUTIONS OF THE NONLINEAR MODELS

We turn now to the nonlinear models defined by Eqs. (2.17) through (2.19). These are equivalent to a set of ordinary differential equations which, for Model 1, are:

$$\beta^2 \sigma' = \frac{v}{\tau} (\lambda \sigma - \Delta) + \kappa^2 \Theta(-x) u + \alpha^2 (u - u_\infty), \quad (4.1)$$

$$\epsilon' = \frac{1}{v\tau} (\lambda \sigma - \Delta), \quad (4.2)$$

$$\Delta' = \frac{1}{v\tau} (\lambda \sigma - \Delta) [1 - \gamma_1 \sigma \Delta], \quad (4.3)$$

$$u' = \sigma + \epsilon. \quad (4.4)$$

To obtain the analogous equations for Model 2, replace $\gamma_1 \sigma$ in the square brackets in (4.3) by $\gamma_2 v \epsilon' = \gamma_2 (\lambda \sigma - \Delta) / \tau$.

We integrate these equations numerically using a twelfth-order predictor-corrector algorithm. The initial conditions are $\sigma = \epsilon = \Delta = 0$ at $x \rightarrow -\infty$, far ahead of the decohesion front. Our strategy is to fix the material parameters λ , γ , and τ (or, equivalently, c , σ_y , and τ), the velocity v , and the strength of the driving springs α^2 , and to adjust u_∞ to obtain a solution with the property that $u(0) = 1$ and $u \rightarrow u_\infty$ as $x \rightarrow +\infty$. Such a solution always exists. Recall that, in our analogy with the crack propagating in a prestressed strip, the parameter u_∞ is analogous to the displacement of the strip edges far ahead of the crack tip. We therefore might think of our procedure as adjusting the driving stress on the strip to achieve a certain velocity of fracture propagation.

Before looking in detail at these solutions, consider the following thought experiment. Imagine that we start with a static, unstressed system and $u_\infty = 0$. Suppose also that the cohesive springs act only for $x < 0$; that is, we arbitrarily disconnect them for $x > 0$. Let us now increase u_∞ from zero quasistatically. In this limit of infinitesimally slow displacement and a fixed position of the decohesion front, the nonlinear models are indistinguishable from the linear model as long as the stress in the membrane nowhere exceeds the plastic yield stress. This is because, for $\sigma < \sigma_y$, the quasistatic system must stay arbitrarily close to the nonflowing state with $\epsilon = \Delta = \lambda \sigma$ and the nonlinear term in (2.6) is irrelevant.

The linear theory tells us that the largest stress occurs at $x = 0$ where, for this quasistatic situation, it has the value $\sigma_{max} = \alpha u_\infty \kappa$. At this point, the displacement of the membrane is $u(0) = \alpha u_\infty / c$. Clearly, the behavior of this system depends sensitively on whether or not σ_{max} exceeds the plastic yield stress σ_y before $u(0)$ reaches the breaking point $u(0) = 1$. Thus the critical value of the yield stress that marks some kind of quasistatic boundary between brittle and ductile behavior of these models is $\sigma_y = \kappa c$.

If $\sigma_y > \kappa c$, then the threshold for propagating decohesion is reached before any plastic flow occurs, and we deduce that both nonlinear models behave much like the linear model for small enough speeds v — i.e. they are “brittle.” On the other hand, if $\sigma_y < \kappa c$, then plastic flow occurs before the leading cohesive spring breaks. In this case, the two nonlinear models behave differently from one another.

In Model 1, plastic flow must begin as soon as the maximum stress reaches the yield stress. As shown in

Fig. 2, the flowing and nonflowing states cross at this point. If u_∞ is increased very slowly beyond this point, just as in conventional models of plasticity, the stress at $x = 0$ remains fixed at σ_y . The displacement $u(0)$ also remains fixed at its value below the decohesion threshold, $u(0) = 1$, because no additional stress can be applied to stretch the cohesive springs. The only thing that can happen is that, as u_∞ continues to grow, the material in the region $x > 0$ deforms plastically. Thus, decohesion is not initiated, but an indefinitely large amount of plastic work is done on the system. We therefore anticipate that the decohesion toughness $K(v)$ for Model 1 must diverge at $v = 0$ whenever $\sigma_y < \kappa c$.

The most interesting questions, of course, have to do with the behavior at nonzero propagation speeds v , where the quasistatic approximations are not necessarily valid. In general, our decohesion criterion $u(0) = 1$ implies that the breaking stress $\sigma(0)$ increases with increasing v . (We shall not consider a stress-based criterion, which might be simpler in some respects.) Actually, at nonzero speeds, the stress reaches its maximum some distance behind the decohesion front. In the linear version of the model, this maximum stress diverges at $v = c$. Thus, even if the maximum stress κc is less than σ_y at $v = 0$, it will become greater than σ_y at some onset speed for plastic flow that we shall call v_p . At speeds larger than v_p , the system must deform plastically.

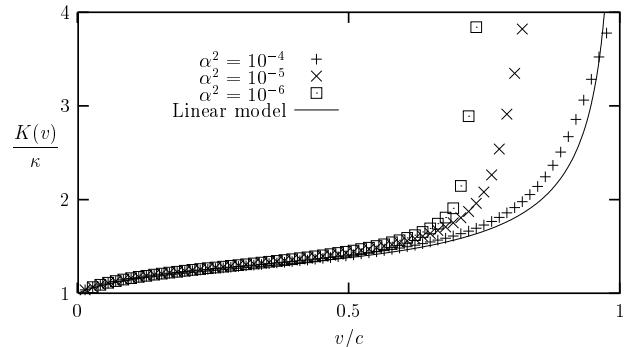


FIG. 5. Decohesion toughness $K(v)$ with $\sigma_c = 3\kappa c$ and $\tau = 10$, for three values of the driving α . The limit of weak driving $\alpha \rightarrow 0$ exists only for $v < v_p \approx 0.73c$.

To see what happens at v_p , we must look at the numerical solutions of Equations (4.1) through (4.3). We continue to consider only Model 1 for the moment. In Fig. 5, we show the decohesion toughness $K(v) = \alpha u_\infty$ as a function of v/c , for $\sigma_y = 3\kappa c$, $\tau = 10$, $\lambda = 1$, and for three different values of α . For comparison, we also show $K(v)$ for the linear theory. The most striking feature is that these four curves are almost coincident for v/c less than a critical value of about 0.73; but they break away from the linear theory at larger speeds, the systems with smaller α being the most dissipative. We see even more explicitly what is happening in Figs. (6) and (7)

where we have plotted the total displacement $u(x)$ and the plastic strain $\epsilon(x)$ for $\alpha = 10^{-3}$, and for two velocities $v/c = 0.71$ and 0.75 , just below and just above the critical speed respectively. Note that the plastic strain is very much larger for the slightly larger value of v . In that case, the plastic strain grows almost linearly with x before it reaches its peak. The spatial extent of the region in which this plastic strain accumulation happens seems to scale linearly with α^{-1} . Note also that decohesion produces a residual plastic deformation and, accordingly, a residual stress (not shown here) that persist infinitely far behind the front.

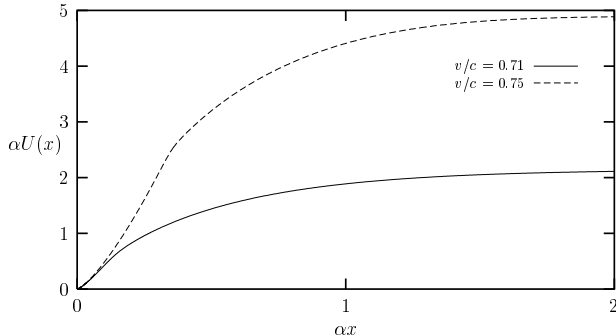


FIG. 6. Total displacement $U(x)$ as a function of x , both measured in units of α^{-1} , for speeds just below and just above v_p . A considerable increase in the driving force αU_∞ is needed to increase the decohesion speed by 4%.

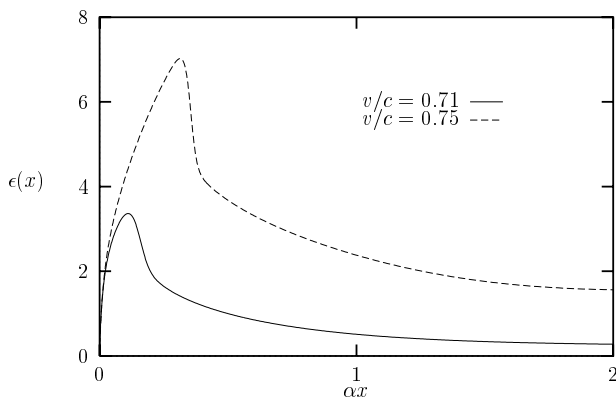


FIG. 7. Plastic strain $\epsilon(x)$ as a function of αx for speeds just above and just below v_p . Note that the peak in $\epsilon(x)$ for $v/c = 0.75 > v_p$ is more than twice that of the peak for $v/c = 0.71 < v_p$, and the level of plastic strain far behind the decohesion front changes by a factor of about 5.

We deduce from this data that the $\alpha \rightarrow 0$ limit exists only for $v < v_p$. That is, if we try to drive decohesion at a speed greater than v_p with springs of arbitrarily small force-constant α^2 , the dissipated energy per unit advance of the front grows without bound. For Model 1,

v_p is the speed at which the maximum stress just exceeds the plastic yield stress. To confirm this interpretation, in Fig. 8 we plot v_p as a function of σ_y and compare this with the prediction of the linear model for the maximum stress

$$\sigma_{max} = \frac{c}{\beta_c} \alpha u_\infty \approx \sigma_y \quad \text{at} \quad v = v_p(\sigma_y), \quad (4.5)$$

where αu_∞ , is given in Eq. (3.17). Agreement with the linear theory becomes exact in the limit of slow decohesion. We can also qualitatively understand the fact that the prediction of the linear model consistently overestimates the onset velocity v_p . When the nonlinear term can be treated perturbatively, it leads to a decrease in the relaxation rate of Δ , since the right hand side of Eq. (4.3) is reduced. The right hand side of the equation for the derivative of the stress (4.1) is therefore increased thus allowing the stress to reach a higher level before the $\alpha^2(u - u_\infty)$ term reverses the sign of σ' . As a result, the maximum stress in a nonlinear system reaches yield at a lower velocity than in the corresponding linear system.

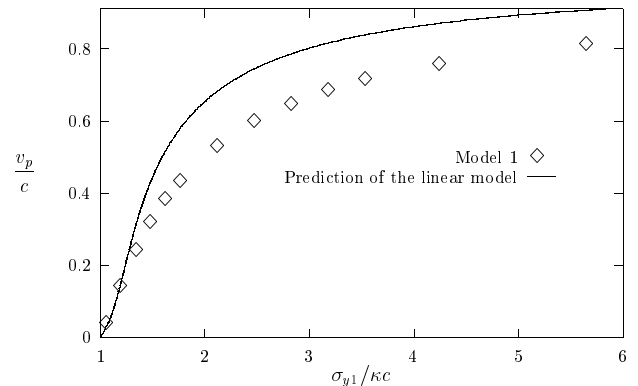


FIG. 8. Onset velocity v_p as a function of the yield stress for Model 1.

So far, we have looked in detail only at the physically less realistic situation in which the plastic yield stress is higher than the breaking stress at the $v = 0$ threshold for decohesion. We now consider the case where the yield stress is lower than the breaking stress. In Model 1, if $\sigma_y < \kappa c$, then we are always in the regime where the $\alpha \rightarrow 0$ limit fails to exist. In examining the behavior in this regime, therefore, we choose a small, fixed value for α , specifically $\alpha = 0.01$, and look at various values of other parameters.

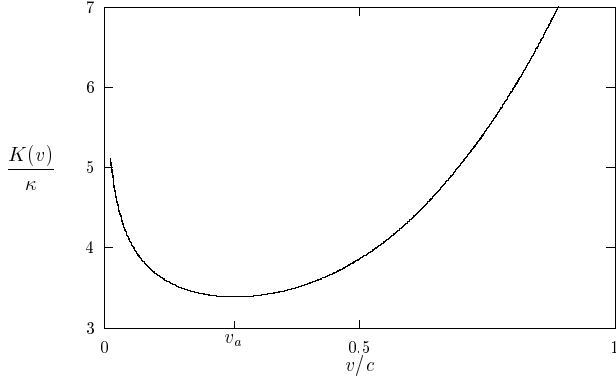


FIG. 9. Decohesion toughness $K(v)$ for Model 1 in the case $\sigma_{y1} = 0.5\kappa c$ for $\alpha = 0.01$.

Fig. 9 is a graph of $K(v)$ as a function of v/c for $\sigma_y = 0.5\kappa c$. The most interesting feature of this graph is that $dK/dv < 0$ for speeds v between zero and, say, v_a . Propagation at speeds in that interval must be unstable; thus, if we increase the driving parameter u_∞ to some value such that $K = \alpha u_\infty > K(v_a)$, then v must jump to some value on the high-speed, stable branch of this curve. Conversely, if we decrease the driving force so that $\alpha u_\infty < K(v_a)$, then decohesion must stop abruptly. As anticipated, the decohesion toughness is large at small speeds because the plastic strain relaxes very slowly near threshold, and the flowing region extends far behind the decohesion front. At larger speeds, the deformation is more localized, and there is less dissipation. At yet larger speeds, of course, the driving force must increase in order to make the front move at speeds comparable to c . To illustrate these variations in the plastic deformation explicitly, in Fig. 10 we plot the plastic strain rate $\dot{\epsilon}$ as a function of x/v . This figure can be interpreted as the plastic strain rate as a function of time after passage of the decohesion front.

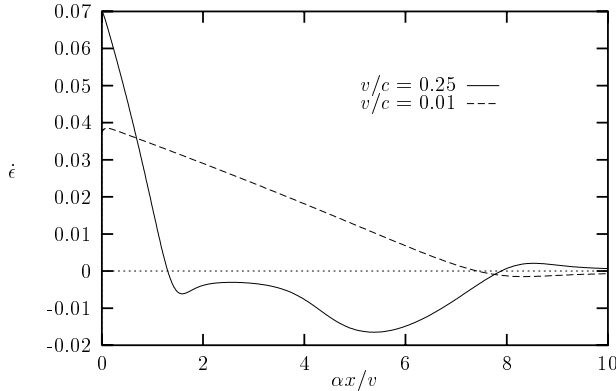


FIG. 10. Plastic strain rate as function of time x/v after the passage of the decohesion front in Model 1. The parameters are the same as in Figure 9. Plastic flow persists much longer for slow decohesion. Also note that plastic strain recovery is appreciable only when decohesion is fast.

We turn now to the properties of Model 2, which must behave in a less conventional manner according to Fig. 3. Even when the breaking stress exceeds the plastic yield stress, $\sigma_y < \kappa c$, the system can remain in the stationary state with $\Delta = \Delta_{2A}$, $\dot{\epsilon} = 0$ so long as the stress is raised sufficiently slowly. No plastic flow occurs, and the decohesion toughness at $v \rightarrow 0$ must be κ , just as in the linear model.

To predict the onset of plastic flow in Model 2, i.e. to compute the analog of $v_p(\sigma_y)$, we can use the linear theory to estimate when the nonlinear term in the equation of motion (4.3) becomes non-negligible. It is useful to carry out this exercise for both models. For Model 1, validity of the linear approximation requires

$$\gamma_1 \sigma \Delta \cong \gamma_1 u'_{el} u'_{pl} \ll 1. \quad (4.6)$$

Our linear analysis tells us that

$$\gamma_1 u'_{el} u'_{pl} \approx \gamma_1 \lambda (\alpha c u_\infty)^2 \left(1 - \frac{v\tau q_1}{1 + v\tau q_1} e^{-x/v\tau} \right). \quad (4.7)$$

This quantity vanishes at the decohesion front, $x = 0$, and rises monotonically to a constant as $x \rightarrow \infty$. We know that $\gamma_1 \lambda = 1/\sigma_y^2$ and, for $\kappa v\tau \ll 1$, $\alpha u_\infty \approx \kappa$. Thus the inequality in (4.6) reduces to $\sigma_{y1} \gg \kappa c$, consistent with our quasistatic analysis for this model.

Model 2 behaves differently. The analog of the inequality (4.6) is

$$\gamma_2 v \epsilon' \Delta \cong \gamma_2 v u'_{pl} u''_{pl} \ll 1. \quad (4.8)$$

From the linear analysis, we find

$$\gamma_2 v u'_{pl} u''_{pl} \approx \gamma_2 v \lambda^2 q_1^3 c^4 \frac{(1 + v\tau q_1)}{(1 + v\tau q_1 c^2)^2} e^{-x/v\tau} \times \left(1 - \frac{v\tau q_1}{1 + v\tau q_1} e^{-x/v\tau} \right). \quad (4.9)$$

Now the nonlinear correction is localized in a finite region whose size is of order $v\tau$ near the decohesion front. We use $\gamma_2 \lambda^2 = 4\tau/\sigma_{y2}^2$. Then, in the case $\kappa v\tau \ll 1$, the inequality (4.8) becomes

$$v\tau \ll \frac{\sigma_{y2}^2}{4\kappa^3}, \quad (4.10)$$

or, equivalently,

$$\frac{\kappa v\tau}{c} \ll \left[\frac{\sigma_{y2}}{2\sigma(0)} \right]^2. \quad (4.11)$$

Both sides of (4.11) are accurate only for $\kappa v\tau \ll 1$. In the opposite limit, $\kappa v\tau \gg 1$, (4.8) reduces simply to $\sigma_{y2} \gg \kappa$. The important point is that, when v is sufficiently small in Model 2, brittle behavior can occur for values of the plastic yield stress σ_{y2} that are smaller than the decohesion stress $\sigma(0)$. The right-hand side of (4.10) gives us an upper bound for $v_p\tau$ for Model 2.

V. DISCUSSION

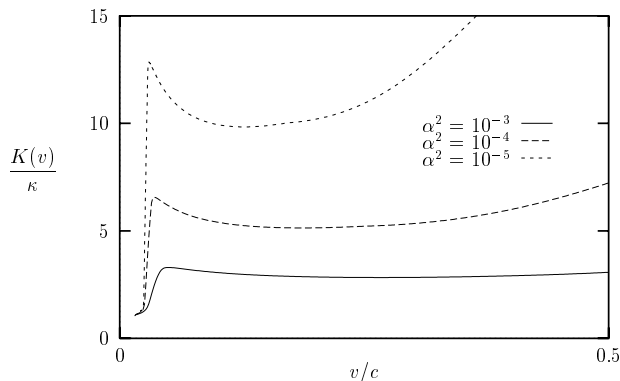


FIG. 11. Decohesion toughness $K(v)$ in Model 2 for three different values of α . Other parameters are $\sigma_{y2} = 0.8\kappa c$, $\lambda = 1$ and $\tau = 4$.

These features of the behavior of Model 2 are confirmed by our numerical results. In Fig. 11, we show the decohesion toughness $K(v)$ as a function of v for $\sigma_{y2} = 0.8\kappa c$ for three different values of α^2 , $\lambda = 1$ and $\tau = 4$. As expected, $K(0) = \kappa$. There is a stable region at small v where $dK/dv > 0$ and in which the limit $\alpha \rightarrow 0$ exists. The onset of plastic flow speed, and the failure of that limit, occurs at $v = v_p$ where $K(v)$ first begins to rise sharply. Beyond its maximum, the fracture toughness in Model 2 behaves qualitatively like Model 1. That is, for small but nonzero values of α , there is an unstable region in which $K(v)$ decreases for increasing v . At yet larger values of v , $K(v)$ rises again and diverges as v approaches c in the limit of $\alpha \rightarrow 0$. As shown in Fig. 12, the plastic flow onset velocity v_p in Model 2 vanishes only as the yield stress σ_y is reduced to zero. Its behavior for small yield stresses is consistent with the prediction of the perturbation theory Eq. (4.10).

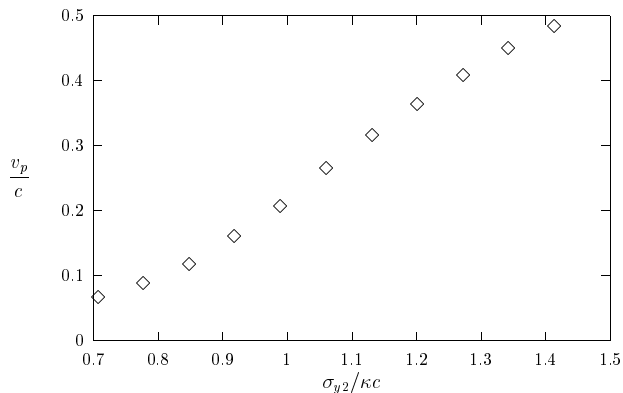


FIG. 12. Onset velocity v_p in Model 2 for $\lambda = \tau = 1$ as a function of the yield stress σ_{y2} . Lower yield stresses are numerically difficult to access.

We have explored these one-dimensional models of decohesion primarily as an attempt to understand how a fully dynamic description of viscoplasticity might play a role in theories of dynamic fracture. We are particularly interested in how the concepts of brittleness and ductility will emerge in such theories.

To begin this discussion, consider one way in which we might expect the brittle-ductile transition to appear in a theory of, say, mode I fracture along the centerline of an infinitely long, two-dimensional strip. Let the width of the strip be $2W$, and suppose that the driving force is produced by a rigid displacement of size u_∞ at its edges. In the case of brittle fracture, the stress-intensity factor at the tip of the crack is proportional to $K_I = u_\infty/\sqrt{W}$. Infinitely far behind the crack tip, the steady-state crack opening displacement is $2u_\infty$. In the limit $W \rightarrow \infty$, K_I remains fixed for a fixed speed of crack propagation, and thus the ratio u_∞/W vanishes. The crack remains sharp and narrow on the macroscopic scale W .

The extreme ductile version of this situation is one in which the solid is replaced by a viscous fluid, and the crack becomes a finger in a Hele-Shaw cell. In this case, the steady-state finger has a width u_∞ of approximately W , and the dissipation rate, proportional to K_I^2 , diverges as $W \rightarrow \infty$. In any real two or three dimensional solid, of course, the plastic yield stress is nonzero. Therefore, as we increase W at fixed crack speed — no matter whether the crack is advancing in a brittle or ductile manner — we must eventually get to the point where the stresses far away from the crack tip drop below the plastic yield stress. The dissipation may become very large, but it remains finite when $W \rightarrow \infty$.

In our one-dimensional model, the closest available analog of the width W is the length scale α^{-1} . However, we have no analog of the stress concentration that is produced by a real second dimension, and thus we have no way in which the far-field stresses can be made arbitrarily small — less than the plastic yield stress — by taking the limit of a large system. In its brittle mode, as we have seen, the analog of the stress-intensity factor for our decohering membrane is $K(v) = \alpha u_\infty \approx u_\infty/W$; this quantity remains finite at fixed v in the limit $\alpha \rightarrow 0$. In its ductile mode, however, our system is behaving more like a finger in a Hele-Shaw cell than a crack in a solid strip. As soon as plastic flow starts at any point, the dissipation rate diverges as $\alpha \rightarrow 0$. In short, the distinction between brittle and ductile failure in this system must be qualitatively unlike that which occurs in real fracture. To understand the latter, we shall have to carry out fully two-dimensional investigations.

What, then, are the lessons to be learned from this exercise? What questions does it raise? We have confirmed, as expected, that the FL model of viscoplasticity produces both brittle and ductile propagating failure modes. In this one-dimensional version, the transition

between brittle and ductile behavior is perfectly sharp and well defined; it is distinguished by the divergence of the decohesion toughness in the limit $\alpha \rightarrow 0$. Is there any such sharp distinction in higher dimensions? The behavior of our one-dimensional models, especially at small propagation speeds v , is strongly sensitive to our choice of the nonlinear coupling between the plastic strain rate and the new variable Δ that describes the internal state of the system. It will be important to learn whether more realistic models in higher dimensions exhibit similar sensitivity to details of the mechanisms that control plastic flow.

Perhaps the most interesting but problematic aspect of our results is related to that sensitivity. Both of the models discussed here exhibit unstable steady-state solutions at low propagation speeds. We know that these solutions are unstable because the decohesion toughness $K(v)$ decreases with increasing v . In both models, $K(v)$ rises again at higher speeds, and the stable high- v solutions are ductile. In Model 2, however, there is also a stable small- v solution that is brittle. That is, there exists a range of values of $K(v)$ for which there are two stable steady-state solutions, one brittle and one ductile. Within such a range of driving forces, the system is likely to exhibit complex, non-steady behavior. What might be the analog of such behavior in two-dimensional models of fracture? Might there be situations in which multiple solutions exist but both are brittle? Or might the slow solution be the ductile one? More generally, might the new dynamics emerging from the FL model of viscoplasticity be a clue for understanding the complex instabilities and different modes of behavior observed in real fracture?

ACKNOWLEDGMENTS

We thank M. L. Falk for many stimulating conversations. This research was supported by DOE Grant No. DE-FG03-84ER45108 and also in part by NSF Grant No. PHY94-07194.

- [7] T. Vu-Khahn and Z. Yu, *Theor. Appl. Fracture Mech.* **26**, 177 (1997).
- [8] L. B. Freund and J. W. Hutchinson, *J. Mech. Phys. Solids* **33**, 169 (1985).
- [9] P. A. Mataga, L. B. Freund, and J. W. Hutchinson, *J. Phys. Chem. Solids* **48**, 985 (1987).
- [10] L. B. Freund, in *Dynamic fracture mechanics* (Cambridge University Press, Cambridge, 1990), Chap. 8.4.
- [11] E. B. Glennie, *J. Mech. Phys. Solids* **19**, 255 (1971).
- [12] M. L. Falk and J. S. Langer, private communication (unpublished).
- [13] M. Barber, J. Donley, and J. S. Langer, *Phys. Rev. A* **40**, 366 (1989).
- [14] M. Marder and S. Gross, *J. Mech. Phys. Solids* **43**, 1 (1995).

-
- [1] J. S. Langer and A. E. Lobkovsky, submitted to *J. Mat. Phys. Solids* (unpublished).
 - [2] A. N. Stroh, *Advances in Physics, Philosophical magazine supplement* **6**, 418 (1957).
 - [3] F. A. McClintock, *J. Appl. Mech.* **35**, 363 (1968).
 - [4] J. R. Rice and R. Thomson, *Phil. Mag.* **29**, 73 (1974).
 - [5] M. F. Ashby and J. D. Embury, *Scripta Metall.* **19**, 557 (1985).
 - [6] C. B. Bucknall, *Toughened plastics* (Applied Science Publishers, London, 1977).